

Low-Temperature Oxidation of Carbon Monoxide with Gold(III) Ions Supported on Titanium Oxide**

Wolfgang Grünert,* Dennis Großmann, Heshmat Noei, Marga-Martina Pohl, Ilya Sinev, Andrea De Toni, Yuemin Wang, and Martin Muhler

Abstract: Au/TiO₂ catalysts prepared by a deposition–precipitation process and used for CO oxidation without previous calcination exhibited high, largely temperature-independent conversions at low temperatures, with apparent activation energies of about zero. Thermal treatments, such as He at 623 K, changed the conversion–temperature characteristics to the well-known S-shape, with activation energies slightly below 30 kJ mol^{−1}. Sample characterization by XAFS and electron microscopy and a low-temperature IR study of CO adsorption and oxidation showed that CO can be oxidized by gas-phase O₂ at 90 K already over the freeze-dried catalyst in the initial state that contained Au exclusively in the +3 oxidation state. CO conversion after activation in the feed at 303 K is due to Au^{III}-containing sites at low temperatures, while Au⁰ dominates conversion at higher temperatures. After thermal treatments, CO conversion in the whole investigated temperature range results from sites containing exclusively Au⁰.

Despite two decades of research on catalysis with supported gold catalysts, there has remained much disagreement with respect to the origin of their remarkable reactivity. Even for a reaction as simple as CO oxidation, the nature of the active sites is still under debate. Regarding the oxidation state of gold in them, most research groups favor the metallic state, in

particular Au⁰ atoms at the perimeter between metal cluster and support surface.^[1,2] Typical mechanisms involve the reaction of CO adsorbed on Au⁰ sites or on slightly positively charged clusters (Au_n^{δ+}) with oxygen activated on the redox active support^[2] or even with support oxygen.^[3] Activation of both reactants by exposed sites of the gold nanoparticles has also been proposed.^[4] It may explain high activities obtained also with Au on irreducible oxides.^[5–7]

The role of Au cations often coexisting with Au⁰ in the most active catalyst states^[8–10] is a matter of debate. In line with earlier work of Schwartz et al.,^[9] we considered them as spectators because upon their complete reduction, a model catalyst containing Au/TiO₂ nanoaggregates hosted in MCM-48 lost only some of its activity.^[10] Models have been proposed in which Au ions at the perimeter between the Au particle and support hold OH groups involved in the oxidation mechanism.^[11,12] Opinions according to which Au³⁺ sites can catalyze CO oxidation alone^[13] or better than Au⁰^[14] are rare, although it has been shown in a theoretical study that Au trimers can catalyze CO oxidation at high rates irrespective of their charge.^[15]

We now present evidence that Au³⁺ sites prepared on TiO₂ by deposition–precipitation (DP) are active for CO oxidation. At the same time, we give an explanation for temperature-independent CO conversion ranges reported for CO oxidation over Au catalysts quite early.^[1] Catalytic CO oxidation by Au³⁺ sites was detected at a temperature as low as 90 K in static regime. In flow experiments, a surface exposing Au³⁺ along with a minority of Au⁰ sites catalyzed CO oxidation well below room temperature with low, sometimes negative apparent activation energies (*E*_{a,app}). Reduction of Au³⁺ to Au⁰ by thermal treatment resulted in a completely different temperature dependence of reaction rates.

4 wt % Au/TiO₂ catalysts were prepared by DP: HAuCl₄ pre-hydrolyzed with a NaOH quantity pre-determined in initial optimization studies^[16] to minimize well-known reproducibility problems with this route^[17,18] was contacted with the TiO₂ surface (Evonik P-25; for details, see the Supporting Information). After Au deposition, the solid was recovered by filtration, washed, freeze-dried overnight, and used for catalytic studies without calcination. If required, this precursor was stored at 255 K in the dark, which did not introduce changes of catalyst behavior beyond the range of scatter experienced in repeated preparations for a duration of up to three weeks.

The catalyst was activated by contact with the feed (1 % CO, 20 % O₂, balance He) at 303 K. After cooling to 215 K in He, a temperature-programmed reaction (TPRe) run was performed (2 K min^{−1} to 303 K, “first run”). Repeated cooling

[*] Prof. W. Grünert, Dr. D. Großmann, Dr. H. Noei, Dr. I. Sinev, Dr. A. De Toni, Dr. Y. Wang, Prof. M. Muhler
Lehrstuhl Technische Chemie, Ruhr-Universität Bochum
P.O. Box 102148, 44780 Bochum (Germany)
E-mail: w.gruenert@techchem.rub.de

Dr. H. Noei

Desy

Notkestrasse 85, 22607 Hamburg (Germany)

Dr. M.-M. Pohl

Leibniz-Institut für Katalyse e.V. an der Universität Rostock
Albert-Einstein-Strasse 29a, 18059 Rostock (Germany)

Dr. A. De Toni

IAV Entwicklungszentrum

Nordhoffstrasse 5, 38518 Gifhorn (Germany)

Dr. Y. Wang

Physikalische Chemie I, Ruhr-Universität Bochum
P.O. Box 102148, 44780 Bochum (Germany)

[**] We gratefully acknowledge financial support by the German Science Foundation (DFG) in the frame of the Collaborative Research Center “Metal-substrate interactions in heterogeneous catalysis” (SFB 558). We thank station scientists of Hasylab (Desy, Hamburg) and Alba (Barcelona) for their engagement during the measurements, and in particular Dr. K. V. Klementiev for his support during pre-commissioning beamtime.



Supporting information for this article is available on the WWW under <http://dx.doi.org/10.1002/anie.201308206>.

in He and TPre resulted in a “second run”, after which the catalyst was subjected to a treatment in He at 623 K (5 K min^{-1} , 30 min isothermal) with subsequent TPre test as described. The series was completed by an analogous treatment in synthetic air at 623 K followed by TPre. For catalysis, a space velocity of $315\,000 \text{ mL g}^{-1} \text{ s}^{-1}$ was used, fourfold that usually applied in literature. Stationary tests were not performed within this study.

Figure 1 shows the typical temperature dependence of CO conversion (X_{CO}). During activation, the catalyst immediately achieved full conversion. In the first run, X_{CO} started with

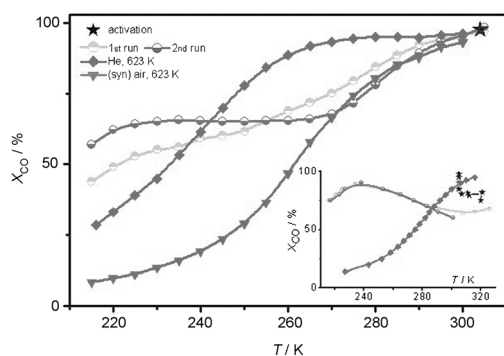


Figure 1. Conversions X_{CO} in CO oxidation over Au/TiO₂ catalyst after different activations. 1% CO, 20% O₂ in He, $315\,000 \text{ mL g}^{-1} \text{ s}^{-1}$. Inset: CO conversions over catalyst prepared in more alkaline medium (see the Supporting Information), 2 wt% Au, measured at $80\,000 \text{ mL g}^{-1} \text{ s}^{-1}$

more than 40% at 215 K and increased with temperature slowly: between 225 and 265 K, $E_{\text{a,app}}$ was estimated as 6 kJ mol^{-1} assuming a rate law that is first-order in CO. Conversion started at about 55% in the second run, but led into a pronounced plateau between 230 and 265 K ($E_{\text{a,app}} = 0$), before it carried on increasing to 100%. Heat treatment resulted in a total change of conversion curves: after activation in He, CO conversion started with less than 30% at 215 K but increased rapidly with temperature. The resulting activation energy of 26 kJ mol^{-1} between 230 K and 265 K is well within the range reported in Ref. [2]. Subsequent air treatment had an adverse effect, though full conversion was still nearly reached at room temperature and there was no significant change in the activation energy (28 kJ mol^{-1} , $255 \text{ K} < T < 280 \text{ K}$).

These patterns were repeated in a number of preparations, although the exact course of the conversion curves was not well reproduced: In a total of seven “first runs”, X_{CO} at 220 K was between 28 and 65% and $E_{\text{a,app}}$ for $220 \text{ K} < T < (260 \pm 10) \text{ K}$ ranged between 6 and 12.5 kJ mol^{-1} , with one exception ($E_{\text{a,app}} = 0$). In a total of six “second runs”, X_{CO} at 220 K was somewhat higher on average ($30\% < X_{\text{CO}} < 75\%$), but developed pronounced plateaus between 220 and $(260 \pm 10) \text{ K}$. As long as the catalyst was not exposed to high temperatures, there were always ranges of very low, zero, or even negative $E_{\text{a,app}}$, while the usual S-shape was obtained after heat treatments. This was even more obvious in an early optimization series^[16] with variation of the NaOH quantity for HAuCl₄ hydrolysis (2 wt% Au, example: inset of Figure 1;

full series: Figure S1). At excess alkalinity, the catalyst deactivated already during activation in the feed. At the same time, the conversion plateaus of subsequent runs became more pronounced or even turned into conversion decay (Figure 1, inset). Such observations suggest that before thermal treatment, CO conversions in different temperature ranges may originate from different sites. Thermal treatments might convert sites operating at low temperatures into different species, which changes the type of the conversion curve.

At different points of the procedure exemplified in Figure 1, the state of the catalyst was investigated by XAFS, TEM, and IR spectroscopy of adsorbed CO: after preparation, namely freeze drying, after the second run, 303 K being the highest temperature in sample history, and after thermal treatments in He and in synthetic air.

The XAFS results confirm the expectation that Au is completely in the +3 oxidation state initially (Figure 2). In EXAFS, there is no indication for either the presence of Au⁰

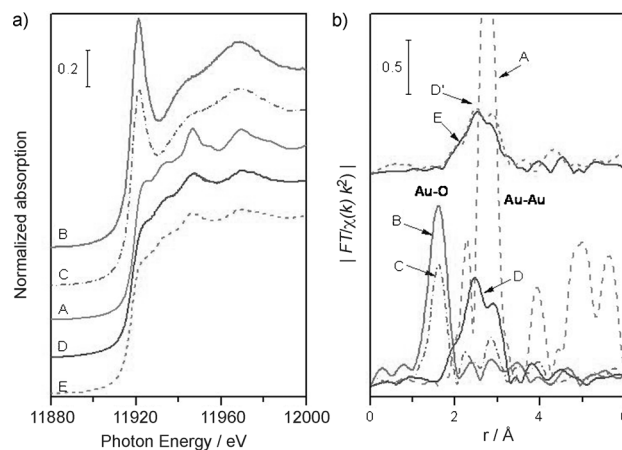


Figure 2. Au L_{III} XAFS spectra: a) near-edge structure (XANES), b) extended X-ray absorption fine structure (EXAFS) of Au/TiO₂ catalyst. A: Au foil, B: initial state (freeze dried), C: after catalysis at $T \leq 303 \text{ K}$, D, D': after thermal treatment in He at 623 K, E: after thermal treatment in synthetic air at 623 K. A–D were measured at 77 K, and D', E at room temperature.

produced by autoreduction^[10] or for higher shells typical of Au oxide or hydroxide phases (Figure 2b). This may indicate ideal atomic dispersion of the gold or the presence of very disordered aggregates. Use of this material in CO oxidation at $T \leq 303 \text{ K}$ caused only a slight reduction of gold (Figure 2a): the XANES of this state was reproduced by linear combination using spectra of the initial state (“I”, 87%) and after He, 623 K (“II”, 13%, Figure S2a). In EXAFS, the Au–O scattering intensity was somewhat decreased (Figure 2b). Intensity in the range of Au–Au⁰ scattering remained low, but could be well reproduced by combining the EXAFS of states I and II in the same 0.87/0.13 ratio (Figure S2b,c). The low reduction degree seems surprising, but is an experimental fact: The sample was taken from a batch showing all reactivity features reported in Figure 1, and possible artifacts during sample preparation for XAFS, storage, and measurement could increase, but never decrease the Au reduction degree.

After thermal treatments, both XANES and EXAFS confirm that gold is completely reduced to the metallic state. In EXAFS (Figure 2b), there is no intensity beyond noise level at distances indicative of O neighbors. The first shell was fitted with an Au–Au distance of 2.82 Å (Table S1, Figure S3; bulk Au –2.87 Å), which indicates the presence of very small Au particles. From the resulting coordination number of 8, a (spherical) particle size of 12–13 Å was estimated using a method described in Ref. [19] This is an illustration rather than an assessment as particles of such size will be hardly spherical. The spectra after treatment in air were identical within experimental accuracy, indicating the presence of exclusively Au⁰.

Microscopic images of the Au/TiO₂ catalyst in different states are presented in Figure 3 and Figure S4. Figure 3a shows the Au atoms in very small disordered patches, and often isolated. Although the patches seem to be two-dimen-

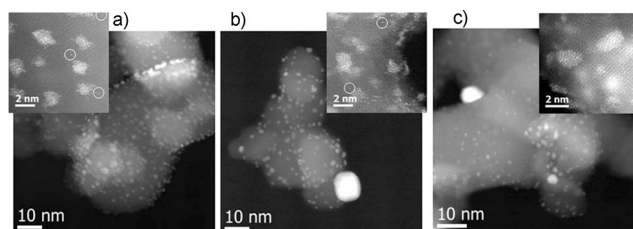


Figure 3. HAADF-STEM images of Au/TiO₂ catalyst a) in the initial state, b) after catalysis at $T \leq 303$ K, and c) after thermal treatment in He at 623 K. Some individual atoms are encircled.

sional, the contrast at TiO₂ particle edges indicates that many of them are in fact three-dimensional. After catalysis at $T \leq 303$ K, the picture is very similar, but additionally some large particles of very different sizes can be found (Figure 3b, Figure S4). Thermal treatment in He seems to produce a similar picture (Figure 3c), but high magnification shows the patches to be ordered and more dense (Figure 3c inset; Figure S4). TEM shows a multitude of particles of about 2 nm size (Figure S4), but there are still particles of less than 2 nm and even single atoms (Figure S4). After air treatment, particles had a more bulky appearance, sometimes with less obvious contact to the TiO₂ surface (Figure S4).

Transmission IR spectra of CO adsorbed onto the initial catalyst at 90 K are shown in Figure 4a. The weak signals are dominated by a band at 2179 cm⁻¹ (CO/Ti⁴⁺),^[20–22] which completely vanishes at very low temperatures (110 K) in accordance with previous work.^[23] There is a shoulder at 2162 cm⁻¹. The related signal, which can be assigned to CO on Au³⁺ sites,^[24] remained after heating to 110 K. Figure 4b shows the response of these signals to the presence of only O₂ in the gas phase. The 2179 cm⁻¹ band decreased and a signal of adsorbed CO₂ at 2341 cm⁻¹, together with carbonate-related bands (not shown) appeared. At the same time, two signals evolved at 2235 and 2256 cm⁻¹ which have not been reported in literature to the best of our knowledge. Obviously, the catalyst was able to catalyze CO oxidation at 90 K already in the initial state. The absence of CO₂ while dosing CO alone

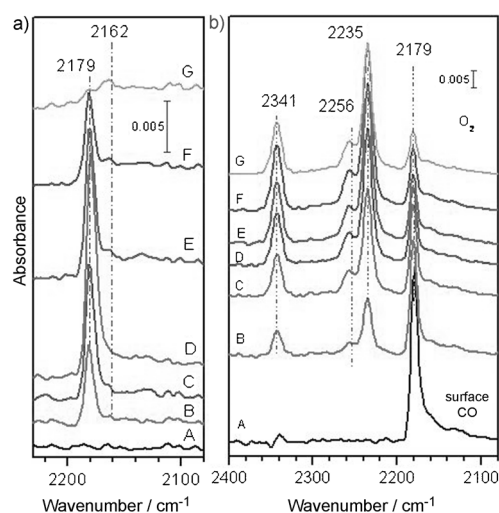


Figure 4. UHV-FTIR spectra of CO adsorbed on Au/TiO₂ in the as-prepared (freeze-dried) state, a) A: clean surface; Adsorption of CO at 90 K and 5×10^{-6} mbar (B), 1×10^{-5} mbar (C), 1×10^{-4} mbar (D); subsequent evacuation at 90 K (E), at 100 K (F), at 110 K (G). b) Interaction between adsorbed CO and gas-phase O₂ at 90 K (A), after adsorption of 4×10^{-4} mbar CO for 21 min; B–G: evacuation and subsequent dosing of 4×10^{-4} mbar O₂ for 7 min (B), 14 min (C), 21 min (D), 28 min (E), 35 min (F), 42 min (G).

for 20 min (Figure 4b, first spectrum) excludes the catalyst as the oxygen source.

To clean the sample from adsorbates, such as possible water remaining after freeze drying, it was heated to 500 K in vacuum. After CO adsorption at 90 K, an intense signal for CO/Au³⁺ was now found at 2158 cm⁻¹, coexisting with CO/Ti⁴⁺ (2179 cm⁻¹) and CO/Au⁰ (2108 cm⁻¹, cf. Ref. [20,21]; Figure S5). At higher temperatures, the former shifted to 2162 cm⁻¹ but was present up to 250 K. From Au⁰, CO desorbed around 150 K,^[15,20,22,24–26] giving sight to another Au-related signal at about 2125 cm⁻¹ (Au_n^{δ+}, cf. Ref. [22]), which was a shoulder of the 2158 cm⁻¹ signal at lower temperatures and persisted until about 200 K.

In Figure 5, the site distribution as reflected by CO adsorption is compared for the remaining catalyst states. After catalysis at $T \leq 303$ K, a strong signal for CO/Au⁰ dominates the spectrum, but a shoulder at 2127 cm⁻¹ (Au_n^{δ+}) and the support signal at 2177 cm⁻¹ can be also discerned. Only partial removal of these bands by thermal desorption allowed observing the signal of CO/Au³⁺ at 2158 cm⁻¹, which persisted until 230 K. While this confirms coexistence of Au³⁺ with Au⁰ sites, site abundances cannot be compared, which is due to a lack of knowledge of extinction coefficients. After He, 623 K (Figure 5b), very strong bands at 2109 cm⁻¹ and 2127 cm⁻¹ (CO on Au⁰ and Au_n^{δ+}) coexisted with the support signal. Now, the region around 2160 cm⁻¹ remained flat even after desorption of CO from the more reduced Au sites: no Au³⁺ was left after the treatment. This holds also for the air-treated sample (Figure 5c), where the shoulder at 2127 cm⁻¹ indicative of Au_n^{δ+} had almost disappeared as well.

Figure S6 shows that all three samples catalyzed CO oxidation at 90 K. The 2235/2256 cm⁻¹ doublet (Figure 4b) no

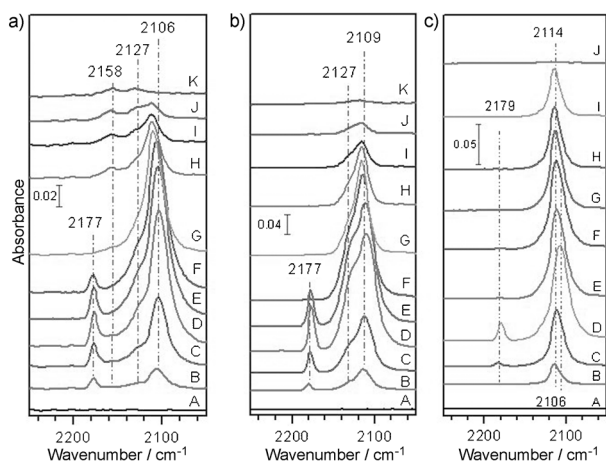


Figure 5. UHV-FTIR spectra of CO adsorbed on Au/TiO₂ in different states. a) after interaction with feed at 303 K, A, clean surface; adsorption of CO at 90 K and 5×10^{-6} mbar (B), 5×10^{-5} mbar (C), 5×10^{-4} mbar (D), subsequent evacuation at 105 K (E), at 120 K (F), at 130 K (G), at 140 K (H), at 170 K (I), at 210 K (J), at 230 K (K); b) after thermal treatment in He at 623 K, A, clean surface, adsorption of CO at 90 K and 5×10^{-6} mbar (B), 5×10^{-5} mbar (C), 5×10^{-4} mbar (D), subsequent evacuation at 90 K (E), at 130 K (F), at 170 K (G), at 190 K (H), at 210 K (I), at 230 K (J), at 250 K (K); c) after thermal treatment in synthetic air at 623 K, A, clean surface; adsorption of CO at 90 K and 1×10^{-6} mbar (B), 1×10^{-5} mbar (C), 1×10^{-4} mbar for 14 min (D), after evacuation at 90 K for 45 min (E), after heating to 110 K (F), 130 K (G), 150 K (H), 170 K (I), 200 K (J).

longer appeared. The capability of Au⁰-containing catalysts to oxidize CO under these conditions is not a surprise, but Figure 4b shows that the same occurs also on a surface where the analysis technique itself rejects the accessibility of Au⁰, on top of the XAFS evidence (Figure 2). The signals at 2235 and 2256 cm⁻¹, which are clearly related to CO₂, were unique for the initial sample. We tentatively assign them to CO₂ subject to H-bond interactions by water remaining adsorbed after freeze drying, which was removed by exposure of the catalyst to higher temperatures. More work will be required to settle this point.

Together with the IR and XAFS evidence, the catalytic data confirm the capability of Au⁰ to catalyze CO oxidation without assistance of Au ions, which do not survive the thermal treatments (Figure 1, Figure 2, Figure 5b,c). Air treatment caused loss of activity (Figure 1), of Au_n^{δ+} clusters, and a looser contact between Au and support (Figure S4). Recent theoretical and experimental studies on methanol oxidation over a Au/TiO₂(110) model catalyst^[27] suggest that these changes may be correlated. After mere activation in the feed, CO conversion at $T < 260$ K is obviously dominated by sites including Au³⁺ ions, which are able to adsorb CO at these temperatures (Figure 5, Figure S5). The very low apparent activation energies can be explained by an established CO adsorption equilibrium. When Au³⁺ no longer holds CO at higher temperatures, sites on coexisting Au_n^{δ+} clusters take over. Depending on their abundance, the CO conversion plateau is more or less extended. The poor reproducibility of conversion levels in this range is apparently due to poor control on the deposition processes used for preparation.

Unfortunately, we cannot decide from our data whether CO conversion in the plateau region arises exclusively from Au ions or from their cooperation with coexisting Au⁰ sites. The static reactivity data from the IR experiment cannot easily be extrapolated into this temperature range. When the initial catalyst was contacted with the feed without activation, CO conversion was low, but clearly significant (1.0–1.3 %) between 170 and 225 K before leaping to 67 % at 250 K and > 95 % at 280 K. It has remained unclear so far if this increase is due to Au⁰ formation^[10] or to removal of remnants from preparation (which caused the low IR intensities from Au sites in the initial state, Figure 4a).

In an recent study with Au deposited on TiO₂ clusters encaged in MCM-48, we failed to observe low-temperature CO oxidation at low or zero activation energies: any activity was created by reduction of Au^{III}.^[10] Obviously, there are more prerequisites for Au^{III} sites to catalyze CO oxidation than only the oxidation state. Strongly negative apparent activation energies of CO oxidation in limited temperature ranges have been reported by Jia et al. for Au/MgO catalysts.^[5] Their origin must be different, because the presence of Au ions in these catalysts is unlikely to be due to the preparation route employed.^[5]

In summary, our data show that TiO₂-supported Au³⁺ ions can catalyze CO oxidation at very low temperatures. Sites consisting of or including Au³⁺ provide CO oxidation rates well comparable with those obtained with Au⁰ clusters, but at very low apparent activation energies (ca. 0 kJ mol⁻¹), probably resulting from the cancellation of the true activation energy and the adsorption enthalpy of CO on Au³⁺ sites.

Received: September 18, 2013

Revised: December 3, 2013

Published online: February 19, 2014

Keywords: active sites · CO oxidation · gold · spectroscopy · titanium dioxide

- [1] M. Haruta, *CATTECH* **2002**, 6, 102–115.
- [2] *Catalysis by Gold* (Eds.: G. C. Bond, C. Louis, D. T. Thompson), Imperial College Press, London, **2006**.
- [3] M. Kotobuki, R. Leppelt, D. A. Hansgen, D. Widmann, R. J. Behm, *J. Catal.* **2009**, 264, 67–76.
- [4] N. Lopez, J. K. Norskov, *J. Am. Chem. Soc.* **2002**, 124, 11262–11263.
- [5] C. J. Jia, Y. Liu, H. Bongard, F. Schüth, *J. Am. Chem. Soc.* **2010**, 132, 1520–1522.
- [6] H. G. Zhu, Z. Ma, J. C. Clark, Z. W. Pan, S. H. Overbury, S. Dai, *Appl. Catal. A* **2007**, 326, 89–99.
- [7] Q. Xu, K. C. C. Kharas, A. K. Datye, *Catal. Lett.* **2003**, 85, 229–235.
- [8] G. J. Hutchings, M. S. Hall, A. F. Carley, P. Landon, B. E. Solsona, C. J. Kiely, A. Herzing, M. Makkee, J. A. Moulijn, A. Overweg, J. C. Fierro-Gonzalez, J. Guzman, B. C. Gates, *J. Catal.* **2006**, 242, 71–81.
- [9] V. Schwartz, D. R. Mullins, W. F. Yan, B. Chen, S. Dai, S. H. Overbury, *J. Phys. Chem. B* **2004**, 108, 15782–15790.
- [10] M. W. E. van den Berg, A. De Toni, M. Bandyopadhyay, H. Gies, W. Grünert, *Appl. Catal. A* **2011**, 391, 268–280.
- [11] G. C. Bond, D. T. Thompson, *Gold Bull.* **2000**, 33, 41–51.

- [12] C. Costello, J. H. Yang, H. Y. Law, Y. Wang, J.-N. Lin, L. D. Marks, M. C. Kung, H. H. Kung, *Appl. Catal. A* **2003**, *243*, 15–24.
- [13] J. C. Fierro-Gonzalez, V. A. Bhirud, B. C. Gates, *Chem. Commun.* **2005**, 5275–5277.
- [14] S. Carrettin, A. Corma, M. Iglesias, F. Sanchez, *Appl. Catal. A* **2005**, *291*, 247–252.
- [15] F. Wang, D. Zhang, X. Xu, Y. Ding, *J. Phys. Chem. C* **2009**, *113*, 18032–18039.
- [16] B. Schumacher, Y. Denkwitz, V. Plzak, M. Kinne, R. J. Behm, *J. Catal.* **2004**, *224*, 449–462.
- [17] A. Wolf, F. Schüth, *Appl. Catal. A* **2002**, *226*, 1–13.
- [18] A. De Toni, Ph.D. Thesis, Bochum **2010**.
- [19] M. Borovski, *J. Phys. IV* **1997**, *7*, C2, 259–260.
- [20] I. X. Green, W. J. Tang, M. Neurock, J. T. Yates, *Science* **2011**, *333*, 736–739.
- [21] J. S. Lee, Z. Zhang, X. Y. Deng, D. C. Sorescu, C. Matranga, J. T. Yates, *J. Phys. Chem. C* **2011**, *115*, 4163–4167.
- [22] M. A. P. Dekkers, M. J. Lippits, B. E. Nieuwenhuys, *Catal. Lett.* **1998**, *56*, 195–197.
- [23] F. Menegazzo, M. Manzoli, A. Chiorino, F. Boccuzzi, T. Tabakova, M. Signoretto, F. Pinna, N. Pernicone, *J. Catal.* **2006**, *237*, 431–434.
- [24] M. Y. Mihaylov, J. C. Fierro-Gonzalez, H. Knozinger, B. C. Gates, K. I. Hadjiivanov, *J. Phys. Chem. B* **2006**, *110*, 7695–7701.
- [25] R. Meyer, C. Lemire, S. K. Shaikhutdinov, H. Freund, *Gold Bull.* **2004**, *37*, 72–75.
- [26] M. Valden, S. Pak, X. Lai, D. W. Goodman, *Catal. Lett.* **1998**, *56*, 7–10.
- [27] M. F. Camellone, J. Zhao, L. Jin, Y. Wang, M. Muhler, D. Marx, *Angew. Chem.* **2013**, *125*, 5892–5896; *Angew. Chem. Int. Ed.* **2013**, *52*, 5780–5784.